lubricants

MDPI

Article

Wear and Friction Reduction on Polyethersulfone Matrix Composites Containing Polytetrafluoroethylene Coated with ZrW_2O_8 Particles at Elevated Temperatures

Andrey I. Dmitriev [1,2,*], Sergei Yu. Tarasov [1], Dmitry G. Buslovich [1], Sergey V. Panin [1], Nikolai L. Savchenko [1], Lyudmila A. Kornienko [1], Evgeny Yu. Filatov [3], Evgeny N. Moskvichev [1] and Dmitry V. Lychagin [4]

1 Institute of Strength Physics and Materials Science, Siberian Branch of Russian Academy of Sciences, 634055 Tomsk, Russia; tsy@ispms.ru (S.Y.T.); buslovich@ispms.ru (D.G.B.); svp@ispms.ru (S.V.P.); savnik@ispms.ru (N.L.S.); rosmc@ispms.ru (L.A.K.); em_tsu@mail.ru (E.N.M.)
2 Department of Metal Physics, National Research Tomsk State University, 634030 Tomsk, Russia
3 Nikolaev Institute of Inorganic Chemistry, Siberian Branch of Russian Academy of Sciences, 630090 Novosibirsk, Russia; decan@niic.nsc.ru
4 Department of Mineralogy and Geochemistry, National Research Tomsk State University, 634030 Tomsk, Russia; lychagindv@mail.ru
* Correspondence: dmitr@ipsms.ru

Abstract

Polymer matrix composites (PMCs) have been prepared having a polyethersulfone (PES) matrix loaded with polytetrafluoroethylene (PTFE) particles coated with negative thermal expansion zirconium tungstate (ZT) with an aim to reduce the thermal mismatch stresses at the PES/PTFE interfaces and, thus, reduce wear rate when sliding against a ball bearing AISI 52100 steel counterpart at elevated temperatures. The zirconium tungsten particles were synthesized using thermal decomposition from hydrothermally prepared precursors. The PMCs have been obtained using compression molding at 370 °C and contained, according to XRD, only the hexagonal α-ZrW_2O_8 phase. Wear testing was carried out at 25, 120, and 180 °C using a ball-on-disk scheme at 5 N and 0.3 m/s. The resulting wear tracks' radial profiles were registered by means of profilometry, which was then used for calculating the wear rate. It was shown that both wear rate and friction reduced in testing the PES/PTFE/ZT samples at 180 °C compared to those of PES/PTFE containing only neat PTFE particles. Wear mechanism transitions have been observed from low-temperature generation of the tribological layer by the PTFE smearing to flow and abrasion wear at high temperatures.

Keywords: polymer matrix composite; negative thermal expansion; zirconium tungstate; wear

check for updates

Received: 18 November 2025
Revised: 3 December 2025
Accepted: 6 December 2025
Published: 9 December 2025

Citation: Dmitriev, A.I.; Tarasov, S.Y.; Buslovich, D.G.; Panin, S.V.; Savchenko, N.L.; Kornienko, L.A.; Filatov, E.Y.; Moskvichev, E.N.; Lychagin, D.V. Wear and Friction Reduction on Polyethersulfone Matrix Composites Containing Polytetrafluoroethylene Coated with ZrW_2O_8 Particles at Elevated Temperatures. *Lubricants* **2025**, *13*, 535. https://doi.org/10.3390/lubricants13120535

Copyright: © 2025 by the authors. Licensee MDPI, Basel, Switzerland. This article is an open access article distributed under the terms and conditions of the Creative Commons Attribution (CC BY) license (https://creativecommons.org/licenses/by/4.0/).

1. Introduction

The influence of thermal expansion on engineering applications, including those involving wear and friction, is an important issue that has gained more interest in recent years. In particular, numerical modeling has shown that this characteristic is important for wear and friction [1,2]. There are also some examples of experimental approaches undertaken in this research area. Purushotham et al. demonstrated that thermal expansion affects the wear resistance of detonation coatings [3]. Superhydrophilic coatings with negative thermal expansion proved to be effective for improving the abrasion resistance of the solar panels [4]. Negative thermal expansion was also effective for devising meta-

and hybrid materials, avoiding high-temperature spallation in them [5]. The efficiency of high-speed train braking depended, among other reasons, on the thermal expansion of the friction blocks [6]. Another publication revealed a relationship between the thermal expansion of the friction block and the braking parameters [7]. The relationship between wear and thermal expansion of AA6082 was studied by Tian et al. [8]. It was shown that thermal expansion affects the contact stress magnitude and localization, which causes the uniformity of wear. The above examples also demonstrate that thermal expansion is important in friction couples composed of metallic materials whose coefficients of thermal expansion (CTE) are of intermediate values between those of ceramics and polymers.

Given that polymers usually possess high CTE, it is especially important to take this into account when devising high-temperature polymer matrix composites (PMCs). The PMCs are used for fabricating structural components in many industries like automotive, aerospace, etc., not only because they help reduce weight and fuel efficiency but also because they demonstrate high impact toughness and thermal stability. High-temperature-resistant and resilient polymers are known, such as polyimides and polysulfones, which make potentially suitable matrices for fabricating the PMCs because of their stability against a wide range of chemicals and durability. For instance, polyetherimide (PEI) and polysulfones (PSU) are frequently used as PMC matrices [9–13].

Polysulfones are amorphous thermoplastic polymers that classify into polyethersulfone (PES) and polyphenylene sulfone (PPSU), which are even more resilient and durable. For example, all three plastics were subjected to end-face sliding against steel both without and with air cooling as well as with sliding in water [10]. Although almost the same wear rates were observed on all samples, plastic deformation was less intensive on the worn surfaces of PPSU samples as compared to those on both PES and PSU. The temperature of water increased from 33–35 to 65–68 as the normal load increased from 25 to 250 N. High coefficient of friction (CoF) values were the reason behind that intensive heating.

PES exhibits excellent long-term thermal endurance, with a continuous service temperature of up to 180 °C. It can withstand short-term exposure to even higher temperatures (exceeding 200 °C), without significant degradation. This stability is fundamentally due to its high glass transition temperature (Tg ≈ 220–225 °C) [11]. PES features a relatively low and linear coefficient of thermal expansion (CTE), typically in the range of 55×10^{-6}/K. This low CTE ensures minimal dimensional change with temperature fluctuations. The material maintains its shape and dimensions under both thermal and mechanical stress. This is a result of its high modulus, low creep tendency, and low moisture absorption, combined with its low CTE. PES possesses high strength and rigidity, with a tensile strength typically ranging from 70 to 85 MPa and a high tensile modulus (approximately 2.5 GPa). This provides excellent resistance to deformation under loading [12].

PES applications include membranes for separation processes like hemodialysis, water filtration, and gas separation, due to its high strength, chemical resistance, and biocompatibility. It is also used in industrial and electrical components that require high heat and chemical resistance, such as pumps, valves, and electrical insulation. Additionally, PES is employed in biomedical engineering for things like surgical instruments, tissue engineering scaffolds, and drug delivery systems [13–15].

PES is widely used for preparing the PMCs by loading it with montmorillonite for improving abrasive resistance [16], carbon fibers [17–20], or perfluorocarbon chains [21]. However, due to its chemical structure, neat PES is subject to intensive wear and, therefore, cannot be used in friction units [22].

Various methods can be utilized to improve the wear resistance of polyethersulfone, including loading with nano- and microfillers, chemical modification, ionizing radiation surface treatment, mechanical activation, etc. [23,24].

The improvement of tribological characteristics of the PMCs can also be achieved with the addition of antifriction substances, which are capable of friction reduction by forming thin superficial films [25]. One of the most commonly used antifriction additives to a PMC would be polytetrafluoroethylene (PTFE) [26,27]. However, its high CTE becomes a problem when a PTFE-containing PMC is subject to friction at elevated temperatures; in this case, the PTFE particles expand and exert high thermal mismatch stress at the PTFE/matrix interface. The CTE may be reduced by depositing a negative thermal expansion (NTE) component, such as, for example, zirconium tungstate ZrW_2O_8 (ZT), onto PTFE particles to be embedded into the PEI matrix [28]. Such a reduction in thermal expansion mismatch stress on the matrix/PTFE interfaces provided a reduction in both wear and friction in sliding a PEI/PTFE/ZT composite against a steel counterpart compared to that of a PEI/PTFE composite. The PTFE films were detected on the worn surfaces of both composites, and this additional friction reduction was provided by the stress relieving rather than antifriction film generation from decomposed ZrW_2O_8, whose volume fraction was as low as 0.5 wt. %. The thermal expansion-controlled wear mechanism was proposed based on thermal expansion of the subsurface PTFE particles, which would cause the sliding surface to bulge. These bulges are subject to severe plastic deformation and/or wear. Reduction in the PTFE particle thermal expansion on account of coating them with finer NTE particles is the reason for improved wear resistance of a PMC containing PTFE whose thermal expansion was tailored by adding an NTE component. Such a result was firstly obtained on the PEI/PTFE/ZT composite and needs to be supported by experimenting with PMCs based on other high-temperature polymers such as polyethersulfones.

It is also known that PTFE has a crystalline component in addition to the amorphous one, depending on the temperature; i.e., it is represented by hexagonal Phase IV in the temperature interval 19–30 °C and pseudohexagonal Phase I above 30 °C when polymer chains accumulate disorder and finally lose their helical repeat unit [29,30]. Therefore, the PTFE capability to form antifriction films on the PMC surfaces during sliding at elevated temperatures may be impaired by degradation of its crystalline component.

In addition to hexagonal structure degradation and thermal expansion [31], stretching deformation during sliding would also have its effect on the subsurface PTFE particles and thus change their crystalline structure [32]. For instance, it is known [33] that the crystallinity of PTFE wear debris is enhanced as compared to that of the original PTFE. All these factors, along with temperature, would affect the wear and friction behavior of the PMCs, including wear mechanism transitions. In particular, the addition of either oxide or ceramic particles to PTFE may modify its antifriction behavior in the rigid polymer matrix. On the one hand, these particles may serve as abrasive ones and thus enhance wear. On the other hand, being fragmented and incorporated in the PTFE film, those particles may serve to reinforce the subsurface layers and make them more stable against wear.

The objective of this study is to compare wear and friction in PES/PTFE and PES/PTFE/ZT composites at elevated temperatures while slid against steel counterparts. Investigate the effect of adding a low concentration of the NTE component on the wear mechanism and degradation of the PTFE antifriction film formation mechanism.

2. Materials and Methods

Thermoplastic PES powder (“Solvay”, Brussels, Belgium) particles with a mean size of ~10 μm and molecular structure as shown in Figure 1a have been used in the preparation of PMCs being filled with fine Fluralit PTFE powder particles (‘Fluralit synthesis’ LLC, Moscow, Russia) (Figure 1b). The mean PTFE particle size was <3 μm as a result of the thermal decomposition of the ‘F-4’ fluoroplastic. The negative thermal expansion additive was a ZrW_2O_8 powder manufactured using thermal decomposition of the

ZrW_2O_7 $(OH)_2 \cdot 2H_2O$ precursor at T = 570 °C. The precursor was prepared by means of hydrothermal synthesis at the Nikolaev Institute of Inorganic Chemistry (Siberian Branch of the Russian Academy of Sciences, Novosibirsk, Russia). More details on the synthesis of ZT particles were reported [34]. The needle-shaped morphology of the ZrW_2O_8 crystallites is shown in Figure 1c,d along with their EDS point elemental composition (Table 1).

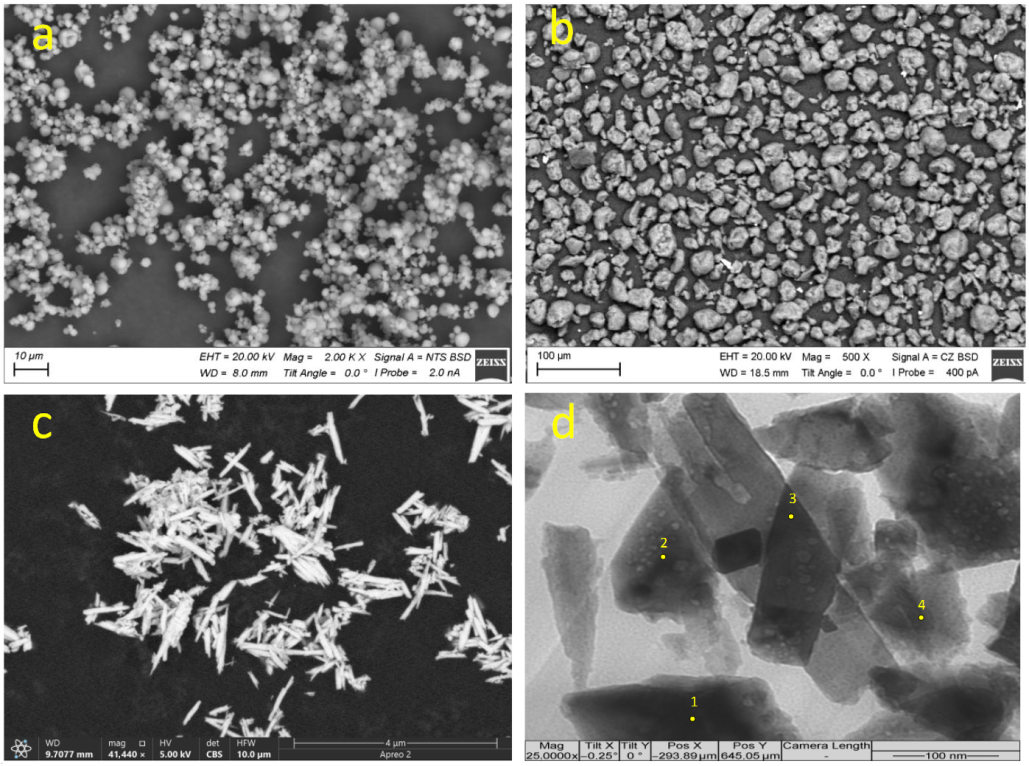


Figure 1. SEM BSD (**a**–**c**) micrographs of as-received PTFE (**a**), PES (**b**) granules, and zirconium tungstate crystallites (**c**). TEM image of ZT particles (**d**) produced by hydrothermal synthesis. The numbers and points identify places where EDS point spectra have been obtained (Table 1).

Table 1. Mean elemental concentrations measured by EDS at points and then averaged for the ZrW_2O_8 particles presented in Figure 1d.

Elements, wt. %/at. %	O	Zr	W
Spectrum 1	32.33/81.94	17.16/7.42	49.61/10.64
Spectrum 2	24.92/75.97	15.25/8.15	59.83/15.87
Spectrum 3	21.24/72.48	13.69/8.20	65.07/19.33
Spectrum 4	9.59/49.23	22.84/20.58	67.57/30.20
Mean percentage	22.24/69.90	17.24/11.09	60.52/19.01
Standard deviation	9.82/14.33	4.0/6.34	7.96/8.27
Max	33.23/81.94	22.84/20.58	67.57/30.20
Min	9.59/49.23	13.69/7.42	49.61/10.64

The next stage was deposition of deagglomerated ZrW_2O_8 particles on the PTFE ones in ethanol with the use of a disperser UZDN-A (UkrRosPribor, Moscow, Russia). The PES particles were then intermixed with either neat PTFE or PTFE/ZT particles using an IKA T18 (IKA-WERKE, Staufen im Breisgau, Germany) disperser, subjected to sonication for 10–15 min by means of an ultrasonic cleaner ('PSB-Gals' Ultrasonic Equipment Center, Moscow, Russia), and again dispersed to provide better intermixing and dispersion of the components (Figure 2). The resulting suspension of particles was dried in an ShS-20-02-SPU drying cabinet (Smolensk SKTB SPU Inc., Smolensk, Russia), followed by milling in an

IKA M20 mill (IKA-WERKE, Staufen im Breisgau, Germany). Compression molding of the powder blends was performed at a pressure of P = 15 MPa and a temperature of T = 370 °C. Finally, the consolidated disk samples were cooled down to room temperature at a cooling rate of 2 °C/min.

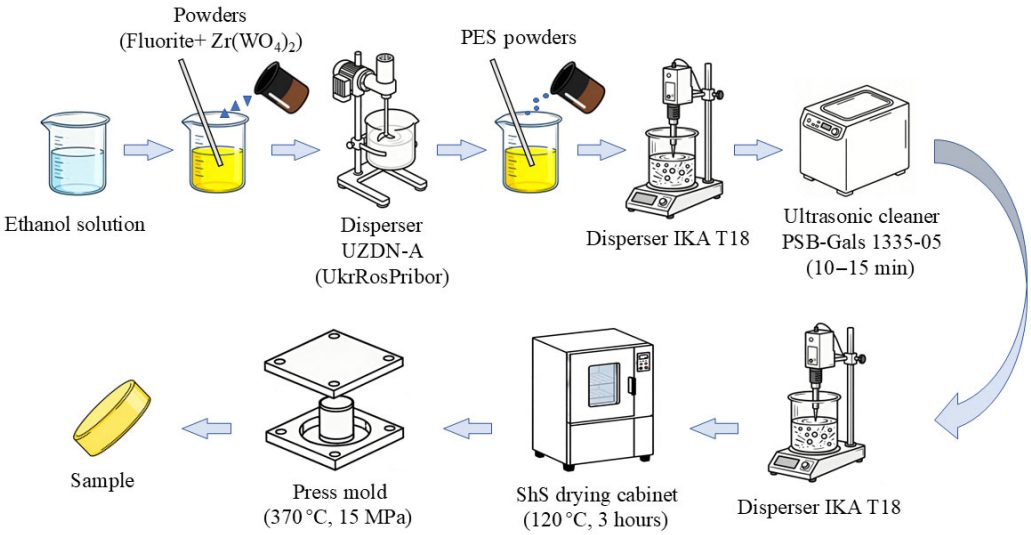


Figure 2. Scheme of the PMC sample preparation.

The resulting PES matrix composites contained (i) 10 wt. % PTFE and (ii) 10 wt. % PTFE + 0.5 wt. % ZT.

A high-temperature tribotester 'THT-S-BE-0000' (CSEM, Neuchâtel, Switzerland) allowed obtaining tribological data with the use of a ball-on-disk (ASTM G99-23) testing scheme at a normal load of P = 5 N and a sliding velocity of V = 0.3 m/s. The total wear path length was L = 1000 m. The counterparts were ∅6 mm AISI 52100 steel 60 HRC balls with R_a = 0.02 µm surface roughness. These parameters ensured obtaining steady friction and wear regimes in sliding at elevated temperatures without any scoring, ploughing, or buckling. The test conditions were similar to those used in our previous studies [25,28].

The maximum Hertzian contact pressure was ~110.2 MPa. The maximum shear stress was 34.2 MPa. The depth of the max shear stress was 0.07 mm. The circular contact area diameter was 0.294 mm.

At least three wear tracks were obtained on each of the PMC samples whose profiles were determined by means of stylus profilometry (KLA-Tencor, Milpitas, CA, USA). The wear track volume loss (V_{loss}) was then assessed by multiplying a circular wear track length (l) by a mean value of wear track cross-section area (S_{cross}) resulting from averaging 10 profiles measured on each of the samples. The wear rate (WR) was then calculated using the following formula:

$$WR = \frac{V_{loss}(\mathrm{mm}^3)}{P(\mathrm{N}) \times L(\mathrm{m})} \quad (1)$$

where P is the normal load, N. L is the total wear path length, m.

The worn surfaces of both AISI 52100 balls and PMC samples were surveyed using optical microscopy ('Neophot 2' optical microscope, Carl Zeiss, Jena, Germany) equipped with a 'Canon EOS 550D' digital camera (Canon Inc., Tokyo, Japan) and an 'Alpha-Step IQ' contact profiler (KLA-Tencor, Milpitas, CA, USA).

The scanning electron microscope (SEM) TESCAN VEGA 3 SBU (TESCAN ORSAY HOLDING, Brno, Czech Republic) with an EDS add-on was applied for examining the sample surfaces preparatory coated with carbon film by means of Quorum Technologies EMITECH K450X (Quorum Technologies, Laughton, UK) equipment.

X-ray diffractograms were obtained using an X-ray diffractometer DRON-8N (Bourevestnik LLC, Saint Petersburg, Russia) with Bragg–Brentano (θ/2θ) focusing and Cu-Kα radiation (λ = 1.54186 Å, 40 kV, 20 mA) in the 2θ range 8–40° with an angle increment of 0.05° and a counting time of t = 20 s. Crystal Impact's software "Match!" (version 3.9, Crystal Impact, Bonn, Germany) was used for XRD peak identification.

3. Results

3.1. Wear of Neat PES

As mentioned in the Introduction section, unfilled PES is not suitable for tribological applications. Specifically, Krasnov et al. [35] introduced the term "antifriction" of polymers as "a ratio between the dispersive component to the overall energy of intermolecular interactions." In addition to the antifriction capacity, the molecular weight of the polymer also influences tribological properties. According to this study [35], polysulfone (an amorphous polymer) and PES from the same family both demonstrate low wear resistance, partly because of their low molecular weight (reduced viscosity). The rationale may be that their molecular structure and strong bonds make them too tough so that no adaptation to severe friction conditions is possible. Additionally, the inclusion of sulfur in PES may serve to enhance its activity and adhesive interaction with the steel counterpart. On the other hand, it is known that the addition of PTFE to PES allows for reducing friction in dry sliding [27]. To avoid ambiguity of experimental results obtained under different testing schemes and conditions and comprehend the wear mechanism of unfilled PES, tribological tests were performed under conditions previously used for polymer matrix composites [28]. The mean coefficient of friction for the metallic counterface was μ = 0.411 ± 0.023 (Figure 3), and the wear was measured as high as 1398.21 ± 17.18 × 10^{-6} mm^3/Nm.

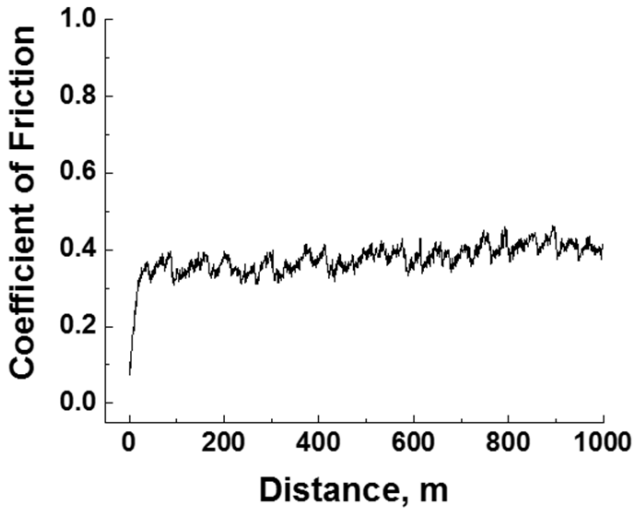


Figure 3. Time dependence of coefficient of friction for neat PES at P = 5 H, V = 0.3 m/s.

Figure 4a,b display images of the steel counterface and PES surface, respectively, along with the profile of the wear track. The PES's worn surface clearly shows deep grooves, even though it has been slid against a smooth surface steel counterface with Ra = 0.02 μm. The worn surface profiling shows a deep circular wear track formed in the PES by a steel counterpart, whose surface is covered by wear debris (Figure 4c) transferred from the PES (Figure 4a). The wear track surface displays rectilinear grooves, which are typical of the adhesive–abrasive wear mechanism (Figure 4b) and likely to be created by the harmful effects of tribo-oxidized PES wear debris (mainly unfixed). To greatly decrease the wear intensity, the contact surfaces need to be "protected" against adhesion wear, which can be accomplished by creating a continuous antifriction tribofilm on the sliding surface of the

PES and by reinforcement of such a transfer film, possibly by adding fine ceramic particles. It was noted above that PTFE is an efficient antifriction polymer whose antifriction capacity comes from the formation of a thin film on the worn surfaces of counterparts. Therefore, it is the best candidate for improving the wear resistance of a resilient polymer matrix.

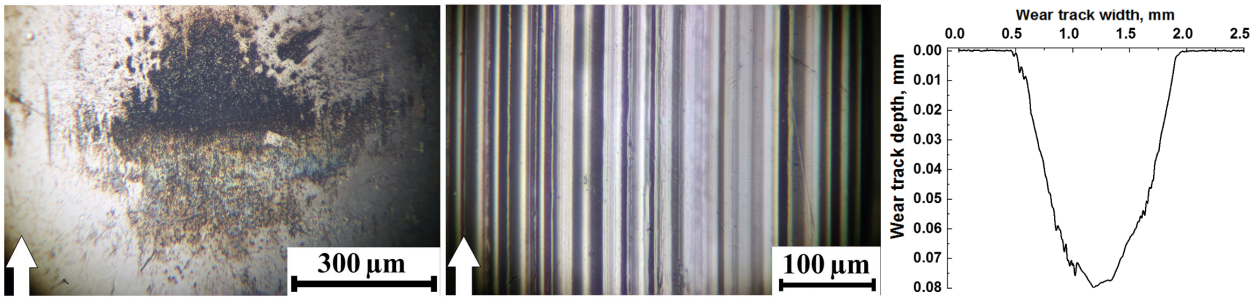


Figure 4. Worn surfaces of steel counterpart (**a**) and neat PES sample (**b**); (**c**) wear track profile.

3.2. Phases and Structures in As-Prepared PMCs

X-ray diffractograms of the as-prepared PMC composites have been obtained, which testify to the crystallinity of the polymer component, attributed to the PTFE particles (Figure 5). The X-ray diffraction peaks were identified as those obtained from a hexagonal crystalline PTFE phase IV, which normally exists in the temperature interval of 19–30 °C [30]. The PES/PTFE/ZT composite additionally demonstrates some small peaks identified as belonging to a hexagonal α-ZrW_2O_8 phase, which is stable in heating up to 155 °C [36] when it transforms to a cubic form, which is also capable of negative thermal expansion. However, it was shown that α-ZrW_2O_8 retains in the PEI even after compression molding at 370 °C since it is known that compression stress serves to stabilize it. The ZrW_2O_8 decomposition temperature is about 770 °C [34].

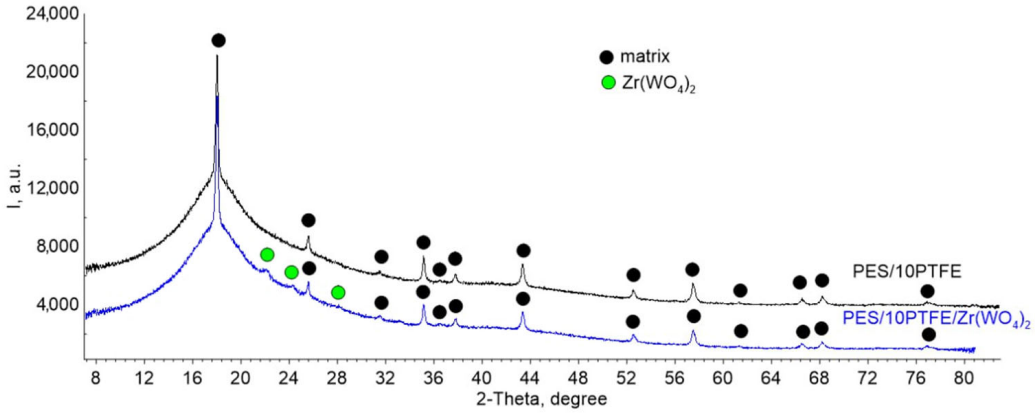


Figure 5. X-ray diffractograms obtained from PES/PTFE and PES/PTFE/ZT.

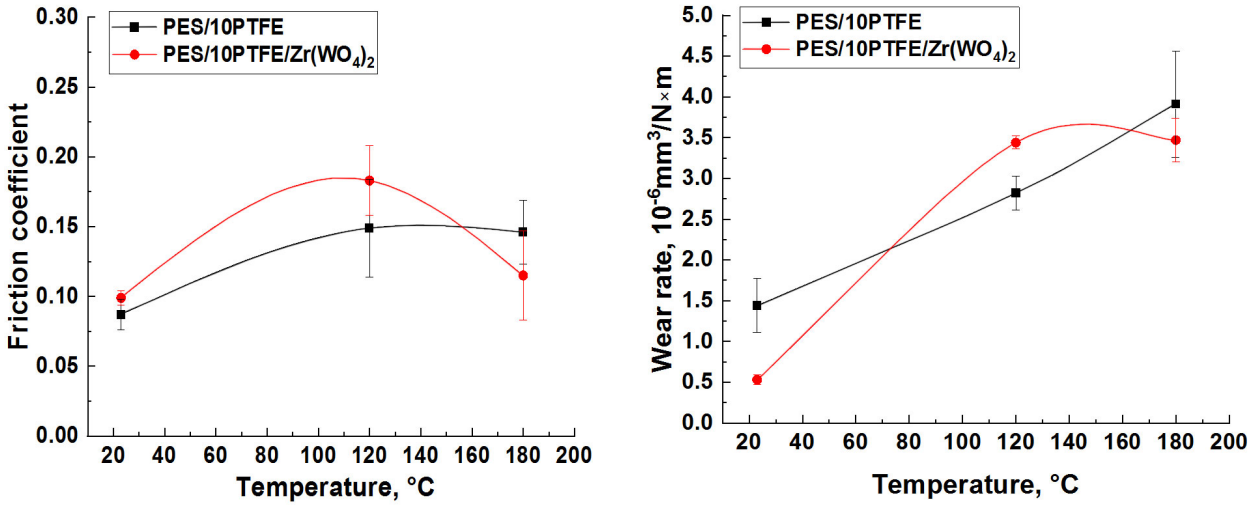
3.3. Wear and Friction Characteristics

The results of tribological testing (Table 2) (Figure 6a) demonstrate that the coefficient of friction (CoF) increases with the test chamber temperature for both types of composites up to the temperature of 120 °C (Table 2, Figure 6a,b). Despite the fact that the CoF values of PEI/PTFE were lower than those of PES/PTFE/ZT in this temperature interval, the most notable friction reduction occurred during sliding on the PES/PTFE/ZT composite at 180 °C. The wear rate of PEI/PTFE increases with temperature almost linearly in the interval of 23–180 °C, while that of PES/PTFE/ZT decreases at 180 °C, much like the CoF (Figure 6b). The addition of 0.5 wt. % ZT resulted in a slight increase in the CoF at 23 and

120 °C; conversely, this allowed for the reduction in the wear rate of PES/PTFE/ZT at 23 °C, followed by an increase at 120 °C to 3.44 ± 0.08 × 10^{-6} mm^3/Nm, compared to 2.82 ± 0.21 × 10^{-6} mm^3/Nm for PES/PTFE. Wear testing results demonstrated that both wear rate (WR) and coefficient of friction (CoF) of the PEI/PTFE/ZT samples decreased during sliding at 180 °C compared to those of PEI/PTFE.

Table 2. Wear test results.

№	Composite	Temperature, T, °C	Coefficient of Friction, *f*	Wear Rate *I*, (10^{-6} mm^3/Nm)
1	PES/PTFE	23	0.087 ± 0.011	1.44 ± 0.33
2		120	0.149 ± 0.035	2.82 ± 0.21
3		180	0.146 ± 0.023	3.91 ± 0.65
4	PES/PTFE/ZT	23	0.099 ± 0.005	0.53 ± 0.06
5		120	0.183 ± 0.025	3.44 ± 0.08
6		180	0.115 ± 0.032	3.47 ± 0.27



(**a**) (**b**)

Figure 6. Coefficient of friction (**a**) and wear rate (**b**) as functions of temperature for PES/PTFE and PES/PTFE/ZT composites.

The CoF dependencies on the wear path length allow for observing that sliding at a room temperature of 23 °C on both PES/PTFE and PES/PTFE/ZT PMCs is characterized by the presence of running-in regimes followed by steady friction regimes (Figure 7a,b). The running-in stages can be observed also in CoF dependencies obtained after sliding at 120 °C, but this time the CoF's behavior is characterized by high-frequency CoF oscillations and some long-time periodicity. The CoF oscillation amplitudes are higher in the case of sliding on PES/PTFE, while longer period CoF intervals are observed for the PES/PTFE/ZT PMC. More steady CoF behavior was obtained during sliding on the PES/PTFE/ZT at 180 °C.

High CoF values and oscillations in testing on the PES composites at 120 and 180 °C may be explained by thermally induced friction enhancement from the PES matrix as well as by unsteady generation and adherence of antifriction films. Sliding at 120 °C on PES/PTFE is characterized by higher unsteadiness as compared to that of PES/PTFE/ZT. This type of unsteadiness is retained during sliding at 180 °C in the path length range of 0–200 m (running-in stage), followed by establishing a long-period oscillation stage. A

similar type of CoF kinetics was observed on the PES/PTFE/ZT, but the running-in stage lasted from 0 to 100 m.

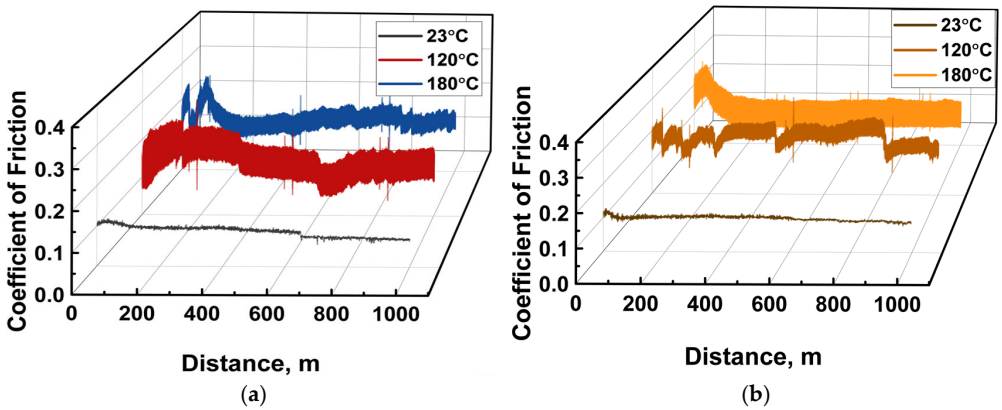


Figure 7. Coefficient of friction vs. wear path distance for (**a**) PES/PTFE and (**b**) PES/PTFE/ZT composites.

3.4. Steel Counterpart's Worn Surface Examination

The optical macrographs of the steel ball's worn surface registered after sliding on both PES/PTFE and PES/PTFE/ZT at 23 °C show dark buildups and shallow (Figure 8a) as well as deep wear grooves (Figure 8a). The worn surfaces of steel balls tested at 120 °C (Figures 8d and 9d) demonstrate deep wear grooves as well as thin patchy films, which appear shiny on PES/PTFE samples tested at 180 °C (Figure 8g). Dark smeared buildups were found on the worn surface of the ball tested at 180 °C against the PES/PTFE/ZT sample (Figure 9g).

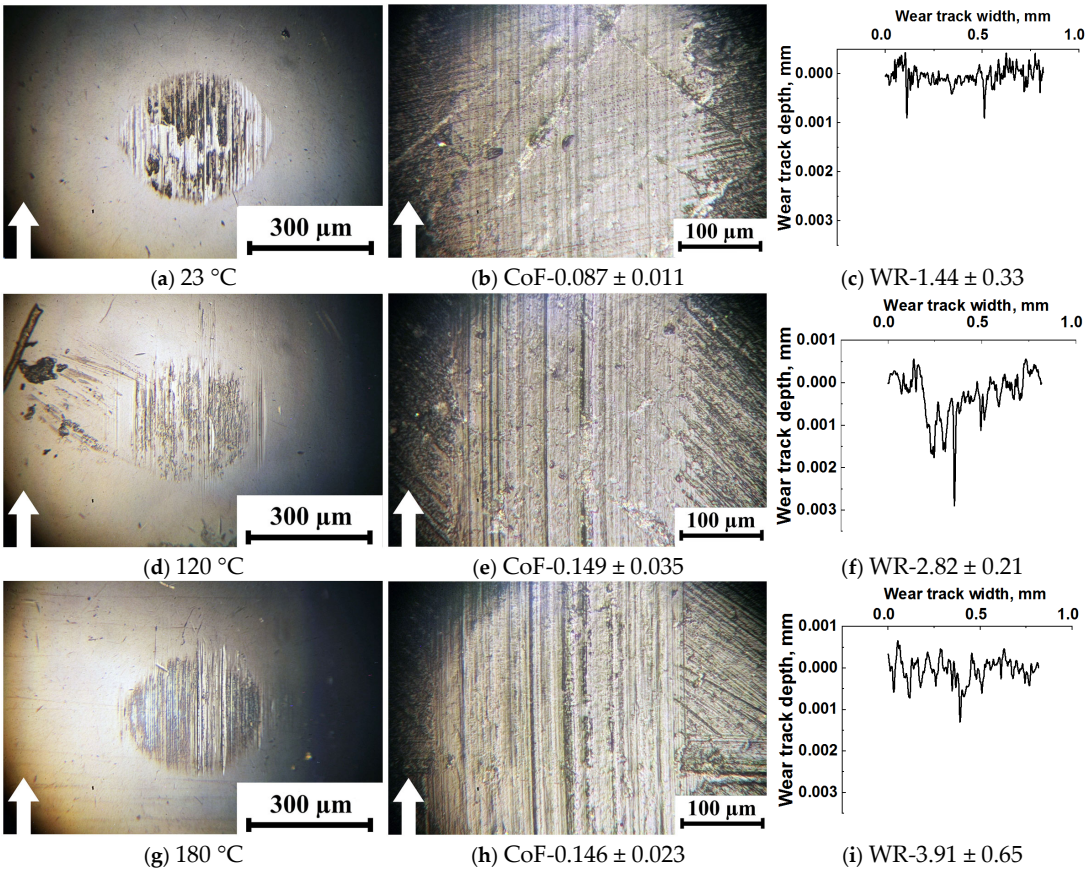


Figure 8. Worn surfaces of steel counterparts (**a**,**d**,**g**) and PES/PTFE (**b**,**e**,**h**) samples; (**c**,**f**,**i**) wear track profilograms.

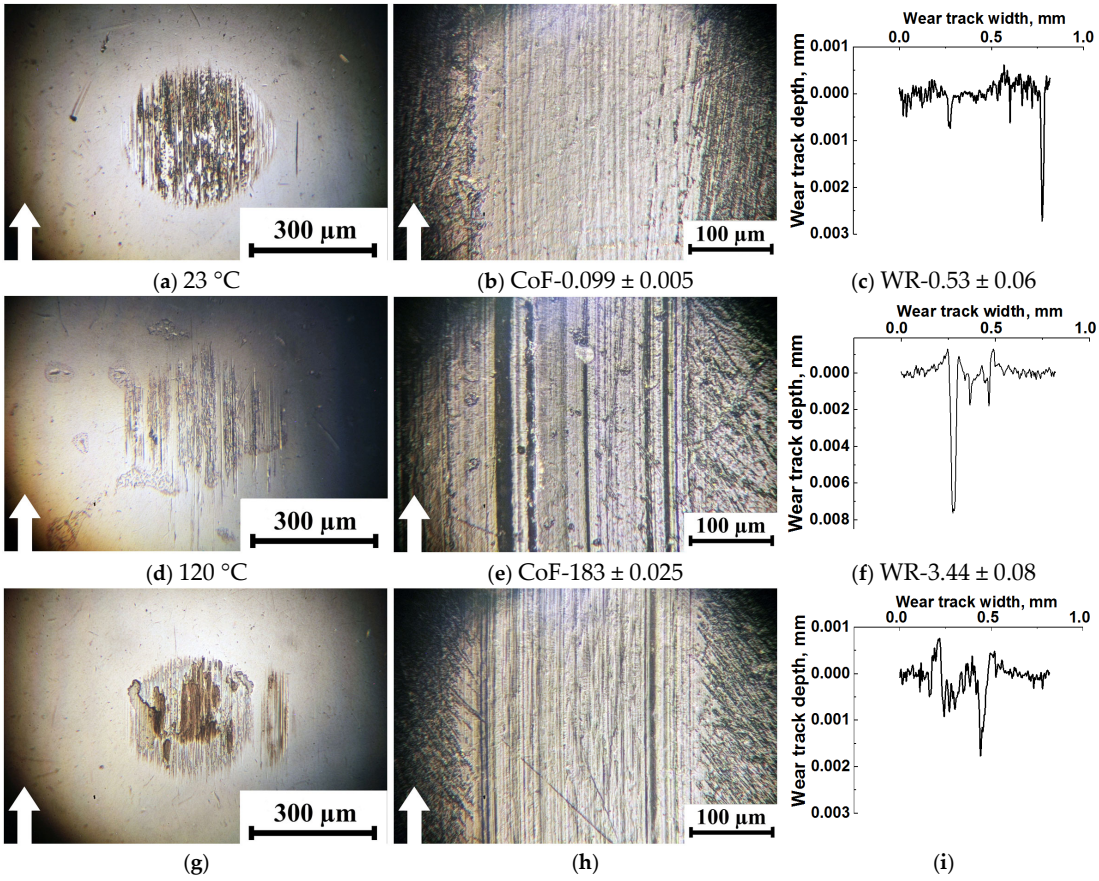


Figure 9. Worn surfaces of steel counterparts (**a**,**d**,**g**) and PES/PTFE/ZT samples (**b**,**e**,**h**); (**c**,**f**,**i**) wear track profilograms.

The PMC's worn surfaces also display both shallow and deep wear grooves (Figures 8b,c,e,f,h,i and 9b,c,e,f,h,i).

The worn surfaces of counterparts demonstrated the presence of transfer films, the amounts of which reduce with increasing the wear rate (Figures 8a,d,g and 9a,d,g). The densest transfer film was generated on the ball tested at T = 23 °C against the PES/PTFE sample, which corresponds to a minimum wear rate of 0.53×10^{-6} mm^3/Nm. In other words, the transfer film proved to be stable on the worn surfaces of both counterparts in the temperature interval from 23 to 180 °C. In addition, sliding at higher temperatures resulted in the formation of deeper wear grooves as compared to those formed at 23 °C, i.e., the adhesive–abrasive wear mechanism by compacted wear particles was aggravated by the temperature.

3.5. PMC's Worn Surface Examination

An SEM image of the worn surface obtained after sliding at 23 °C on the PES/PTFE/ZT composite (Figure 10a) demonstrates the presence of a tribological layer composed of smeared PTFE and ZT particles (Figure 10b–e). The worn surfaces resulting from sliding at 120 °C represent smooth areas with grooves (Figure 11a) covered by PTFE/ZT refined fragments (Figure 11b–e). The dark areas in the sulfur maps (Figures 10f, 11f, and 12f) coincide with those depicting PTFE/ZT particles in Figures 10b and 11b. The generation of smooth film is typical of sliding on PMCs containing antifriction PTFE components under room temperatures [37].

In contrast to the above-described results, the worn surface of the PES/PTFE/ZT sample tested at 180 °C (Figure 12a) acquired a wavy morphology with numerous overlapping shallow wear grooves and wear particles. Such a worn surface morphology is characteristic

of the abrasive wear mechanism. The presence of PTFE/ZT particles (Figure 12b–e) is observed in the form of wear particles smeared over the worn surface against the background of EDS sulfur maps representing the PES matrix (Figure 10f).

The PES/PTFE/ZT composite displayed a dependence of the wear mechanism and corresponding worn surface morphology on the sliding test temperature. Sliding at room temperature is characterized by severe plastic deformation and the formation of PTFE/ZT patchy films, while at 120 °C, deep and narrow wear grooves alternate with smooth areas. Sliding at 180 °C resulted in the formation of the worn surface morphology with numerous shallow grooves. No tribological layer can be observed on this sample, since wear is intensive and rather removes away the superficial layer instead of smearing and intermixing it with the wear particles. It seems that fragmented ZT particles are distributed over the worn surface and thus reinforce it against wear.

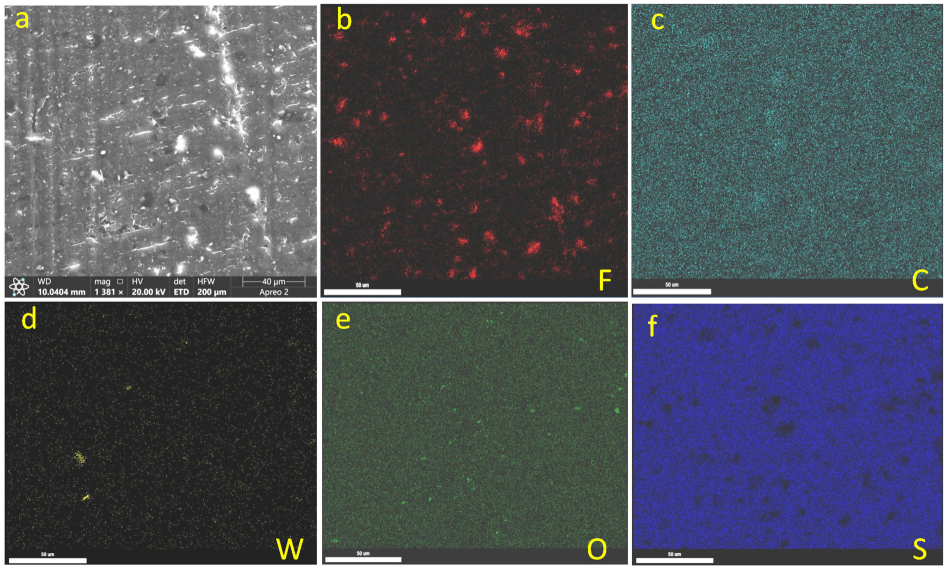


Figure 10. SEM SE image of worn surface (**a**) and corresponding EDS element maps (**b**–**f**) for PES/PTFE/ZT sample tested at 23 °C.

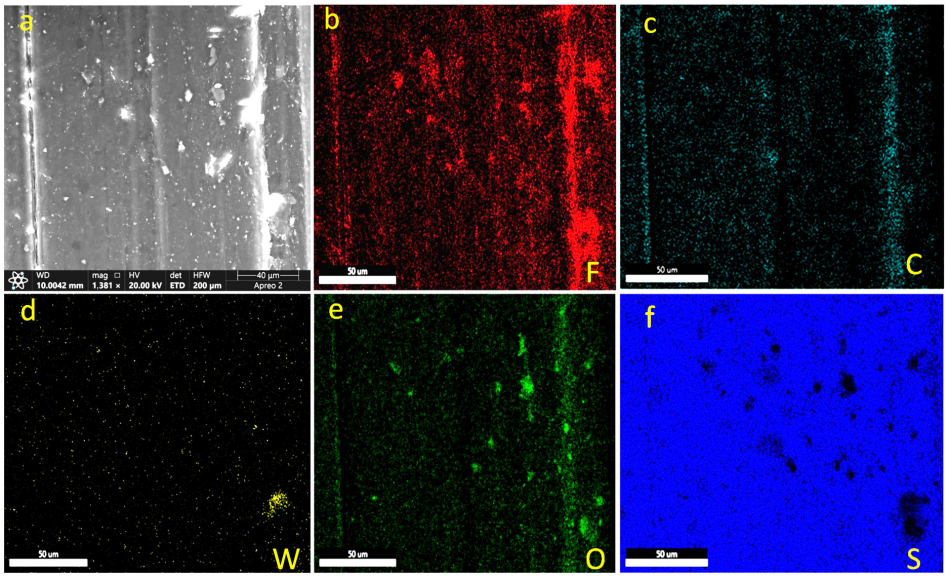


Figure 11. SEM SE image of worn surface (**a**) and corresponding EDS element maps (**b**–**f**) for PES/PTFE/ZT sample tested at 120 °C.

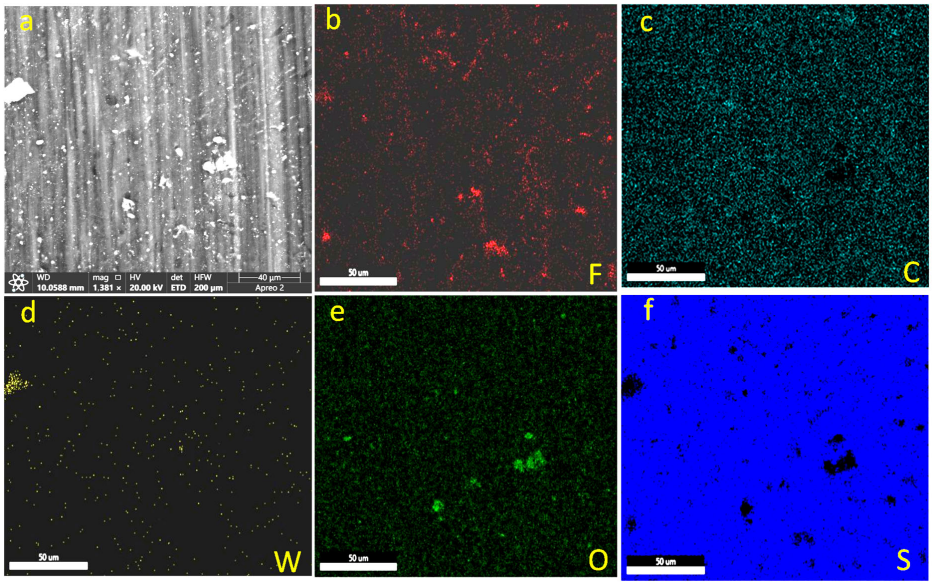


Figure 12. SEM SE image of worn surface (**a**) and corresponding EDS element maps (**b**–**f**) for PES/PTFE/ZT sample tested at 180 °C.

The ZT-free composites tested at 23 °C (Figure 13a–d) demonstrate PTFE particles, discontinuities, and film edges. Several oxidized particles can be seen on the worn surfaces (Figure 13d). The morphology of this worn surface is almost similar to that demonstrated on the PES/PTFE/ZT composite after sliding at the same temperature (Figure 10a–f).

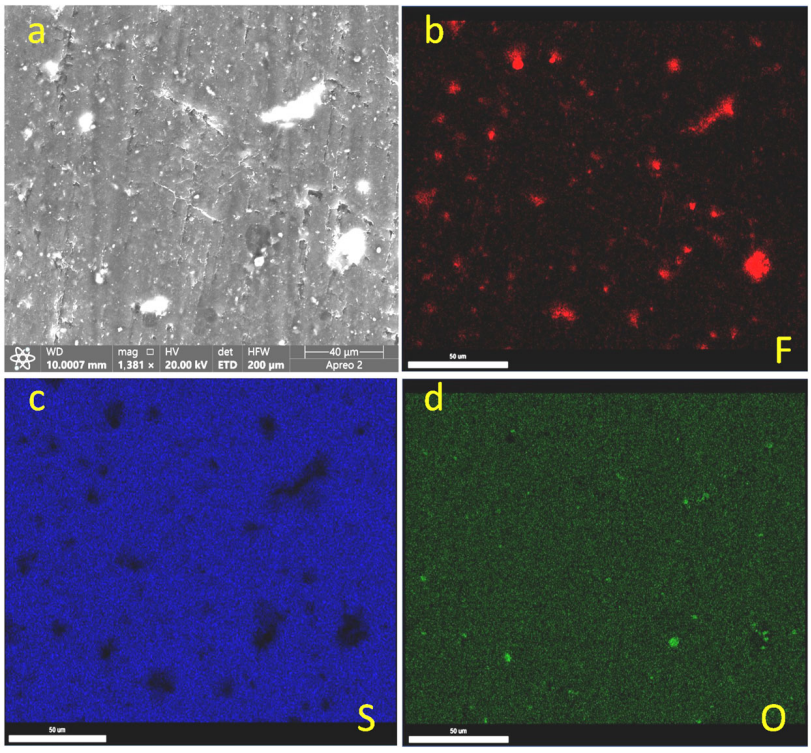


Figure 13. SEM SE image of worn surface (**a**) and corresponding EDS element maps (**b**–**d**) for PES/PTFE sample tested at 23 °C.

PES/PTFE samples tested at 120 °C (Figure 14a–d) demonstrate their worn surface, which is less smooth than that of the PES/PTFE/ZT one (Figure 10a) but also has deep grooves and ZT particles on the background of the sulfur map (Figure 13b–d).

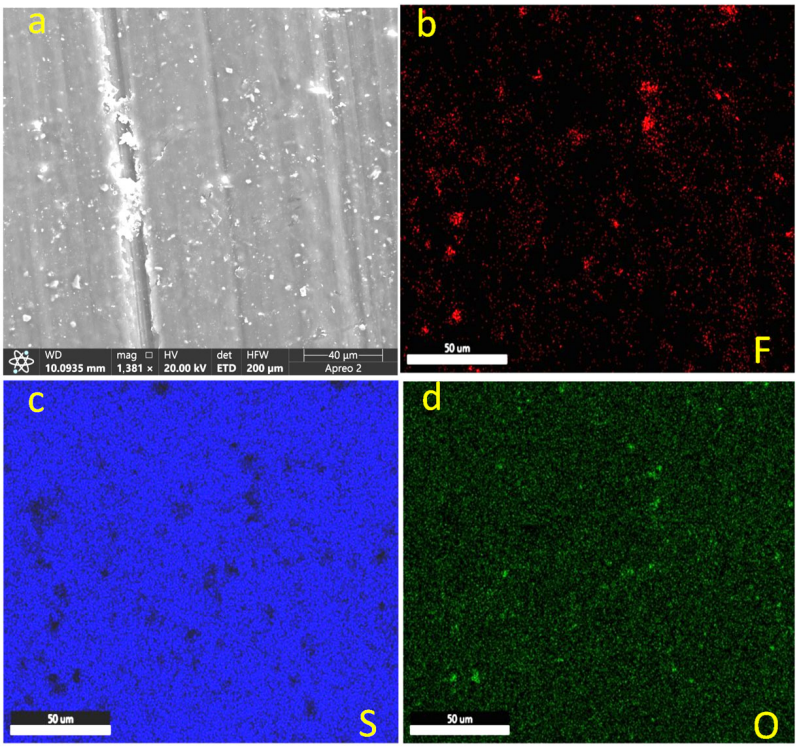


Figure 14. SEM SE image of worn surface (**a**) and corresponding EDS element maps (**b**–**d**) for PES/PTFE sample tested at 120 °C.

The worn surface morphology obtained after sliding at 180 °C (Figure 15a) is almost similar to that of the PES/PTFE/ZT sample tested at 180 °C (Figure 12a); however, it is characterized by deeper wear grooves and areas covered by shallow ones. The PTFE elements, such as fluorine and oxygen, are distributed over the worn surface (Figure 15b–d).

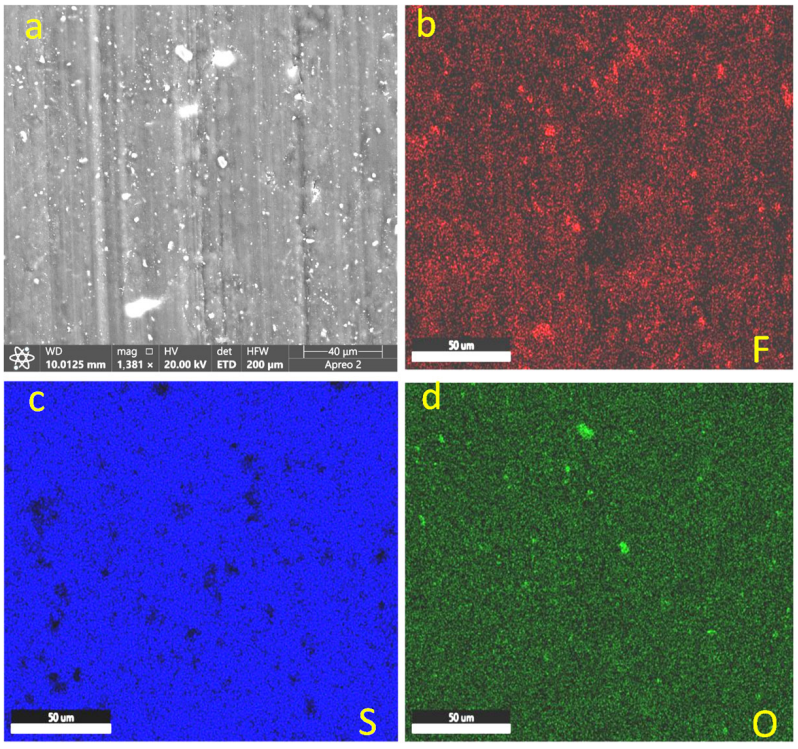


Figure 15. SEM SE image of worn surface (**a**) and corresponding EDS element maps (**b**–**d**) for PES/PTFE sample tested at 180 °C.

The EDS maps testify that more intensive intermixing and element transfer occur over the worn surface with an increase in temperature. At the same time, no traces of iron were detected on the worn surfaces of all samples.

4. Discussion

Polymer matrix composites with the PES matrix and filled with either PTFE or PTFE/ZT particles were obtained, and their tribological behavior was investigated in sliding against steel counterparts at temperatures of 23, 120, and 180 °C. The results of the experiments testified that coefficients of friction of both composites increased in testing from 23 °C to 120 °C. It is also a fact that PES/PTFE/ZT composites showed a lower wear rate in sliding at 180 °C as compared to that of PES/PTFE.

Previous and even more pronounced wear reduction was obtained on PEI/PTFE/ZT composite containing the same amount of PTFE/ZT additive [28]. This wear reduction was related to the purely mechanical effect of thermal stress reduction due to introducing an NTE compound. At the same time, less attention had then been paid to wear mechanisms and the generation of antifriction PTFE/ZT films.

It is reasonable to suggest that the same effect of thermal stress reduction between the PTFE/ZT and PES matrix occurs in sliding at elevated temperatures in PES/PTFE/ZT composites. At the same time, polyethersulfones contain sulfur and therefore are potentially more prone to the tribochemical interaction with oxygen and iron coming from air and steel counterparts, respectively, at elevated temperatures. The presence of the Fe-S-O compound is highly anticipated on the worn surfaces of the composites tested at elevated temperatures since tribochemical reactions between iron and in situ-formed SO_2 were reported [38]. However, it was noted above that no traces of iron were detected on the composites after sliding at all temperatures. The explanation for this fact may be that a tribological layer formed almost completely on the steel counterparts so that sliding occurred between the PMC and the tribologically modified PMC adhered to the steel counterpart surface. The adhesion of the tribological layer to the steel surface is strong enough since no reverse transfer of this layer is observed. It may happen that Fe-S-O chemical bonds contribute to this adhesion.

The composite's worn surface evolution with the test temperature looks almost similar to that demonstrated by the PES/PTFE/ZT composite, i.e., from patchy films to deep grooves alternating with smooth areas and then to wavy patterns with or without deep grooves. Therefore, there is a difference in the worn surface morphology between PES/PTFE/ZT and PES/PTFE composites that is most clearly observed in samples tested at 120 and 180 °C. The worn surfaces of the PES/PTFE/ZT tested at 120 °C are characterized by deep grooves alternating with smooth areas, while those of PES/PTFE demonstrate deep grooves alternating with shallow grooves. The worn surfaces obtained after sliding at 180 °C look similar on both types of composites, with the exception that those on PES/PTFE still have some grooves deeper than those on PES/PTFE/ZT.

It is clear that deep grooves are formed by scratching the worn surface with harder wear particles, which form by means of compacting the wear debris during sliding. On the other hand, shallow grooves are the result of instability of plastic deformation whose contribution is increased with the temperature. Addition of ZT particles resulted in the formation of less deep wear grooves at elevated temperatures. Such a finding may be due to the above-mentioned effect of thermal stress reduction at the matrix/filler interface and, therefore, generation of smaller wear debris. The ZT particles disintegrate into small fragments and even may react with the PES subject to thermal and strain degradation. It is possible that the result of such an interaction will be the formation of W-S compounds, including WS_2, which is a well-known solid lubricant.

In this connection, reinforcement of the composite by ZT particle fragments serves to improve stability of the composite subsurface layer against plastic flow and wear.

5. Conclusions

Polymer matrix composites were fabricated by compression molding, which combined a polyethersulfone matrix with polytetrafluoroethylene/zirconium tungstate particles intended for improving the wear resistance of the composite in sliding against a steel counterpart at elevated temperatures. Wear testing demonstrated that both wear rate and friction reduced in sliding of the PES/PTFE/ZT composite at 180 °C as compared to sliding of the ZT-free PES/PTFE composite. Increasing the test temperature resulted in a wear mechanism transition from low-temperature generation of a tribological layer by the PTFE smearing to flow and abrasion wear at high temperatures.

Author Contributions: Conceptualization, S.Y.T. and S.V.P.; methodology, N.L.S., A.I.D. and D.G.B.; software, N.L.S. and D.V.L.; validation, D.V.L. and L.A.K.; formal analysis, E.Y.F. and L.A.K.; investigation, D.G.B., E.N.M., N.L.S. and E.Y.F.; resources, E.Y.F. and S.V.P.; data curation, D.G.B., N.L.S. and L.A.K.; writing—original draft preparation, S.Y.T.; writing—review and editing, S.Y.T., S.V.P. and A.I.D.; visualization, E.N.M.; supervision, S.V.P.; project administration, S.V.P. and A.I.D.; funding acquisition, S.V.P. and A.I.D. All authors have read and agreed to the published version of the manuscript.

Funding: This research was carried out according to State Assignment for ISPMS SB RAS projects No. FWRW 2022-0004 and FWRW 2021-0010.

Data Availability Statement: Data will be made available on request.

Acknowledgments: The investigations have been carried out using the equipment of Share Use Center "Nanotech" of the ISPMS SB RAS and the core facility "Structure, mechanical and physical properties of materials" at Novosibirsk State Technical University.

Conflicts of Interest: The authors declare no conflicts of interest.

Abbreviations

The following abbreviations are used in this manuscript:

PMC	Polymer matrix composite
PES	Polyethersulfone
PTFE	Polytetrafluoroethylene
ZT	Zirconium tungstate
CTE	Coefficient of thermal expansion
NTE	Negative thermal expansion
CoF	Coefficient of friction
WR	Wear rate

References

1. Grigoriev, A.; Shilko, E.; Dmitriev, A.; Tarasov, S. Suppression of wear in dry sliding friction induced by negative thermal expansion. *Phys. Rev. E* **2020**, *102*, 042801. [CrossRef] [PubMed]
2. Grigoriev, A.S.; Shilko, E.V.; Dmitriev, A.I.; Tarasov, S.Y. Modeling Wear and Friction Regimes on Ceramic Materials with Positive and Negative Thermal Expansion. *Lubricants* **2023**, *11*, 414. [CrossRef]
3. Purushotham, N.; Parthasarathi, N.L.; Suresh, B.P.; Sivakumar, G.; Rajasekaran, B. Effect of thermal expansion on the high temperature wear resistance of Ni-20%Cr detonation spray coating on IN718 substrate. *Surf. Coat. Technol.* **2023**, *462*, 129490. [CrossRef]
4. Deng, W.; Wang, W.; Chen, J.; Zhao, S.; Gu, W.; Nan, J.; Ji, Y.; Xia, Y.; Mao, Z.; Zhu, L.; et al. Negative expansion induced anti-abrasive self-cleaning coatings for enhancing output of solar panels. *Chem. Eng. J.* **2024**, *499*, 156153. [CrossRef]

5. Pasternak, E.; Dyskin, A. Negative Thermal Expansion Realized by an Incomplete Bimaterial Ring. *Phys. Status Solidi B* **2024**, *261*, 2400048. [CrossRef]
6. Deng, S.; Xiang, Z.; Zhang, Q.; Wang, H.; Feng, S.; Yu, Z.; Mo, J. Effect of friction block thickness on the high-temperature tribological behavior of the braking interface of high-speed train. *Tribol. Int.* **2025**, *201*, 110232. [CrossRef]
7. Chen, X.; Lu, C.; Liu, X.; Sun, T.; Mo, J. The influence of competition between thermal expansion and braking parameter on the wear degradation of friction block. *Tribol. Int.* **2024**, *192*, 109246. [CrossRef]
8. Tian, Y.; Kalifa, M.; Khan, M.; Yang, Y. Interplay Between Wear and Thermal Expansion in 6082 Aluminum: A Simulation and Experimental Study. *Appl. Sci.* **2024**, *14*, 10852. [CrossRef]
9. Tu, F.; Wang, B.; Zhao, S.; Liu, M.; Zheng, J.; Li, Z.; Hu, C.; Jiang, T.; Zhang, Q. Synergistic Enhancement Effect of Polytetrafluoroethylene and WSe_2 on the Tribological Performance of Polyetherimide Composites. *Lubricants* **2025**, *13*, 44. [CrossRef]
10. Duan, Y.; Cong, P.; Liu, X.; Li, T. Comparative Study of Tribological Properties of Polyphenylene Sulfide (PPS), Polyethersulfone (PES), and Polysulfone (PSU). *J. Macromol. Sci. Part B Phys.* **2009**, *48*, 269–281. [CrossRef]
11. Sherif, G.; Chukov, D.; Tcherdyntsev, V.; Torokhov, V. Effect of Formation Route on the Mechanical Properties of the Polyethersulfone Composites Reinforced with Glass Fibers. *Polymers* **2019**, *11*, 1364. [CrossRef]
12. Sen Du, S.; Li, F.; Xiao, H.M.; Li, Y.Q.; Hu, N.; Fu, S.Y. Tensile and flexural properties of graphene oxide coated-short glass fiber reinforced polyethersulfone composites. *Compos. Part B Eng.* **2016**, *99*, 407–415.
13. Oprea, M.; Pandele, A.M.; Enachescu, C.I.; Antoniac, I.V.; Voicu, S.I.; Fratila, A.M. Crown Ether-Functionalized Polyethersulfone Mem-branes with Potential Applications in Hemodialysis. *Polymers* **2025**, *17*, 2184. [CrossRef] [PubMed]
14. Wasyłeczko, M.; Wojciechowski, C.; Chwojnowski, A. Polyethersulfone Polymer for Biomedical Ap-plications and Biotechnology. *Int. J. Mol. Sci.* **2024**, *25*, 4233. [CrossRef]
15. Feng, Y.; Chung, T.-S. Fabrication and applications of polyethersulfone hollow fiber membranes. *Hollow Fiber Membr.* **2021**, 315–332. [CrossRef]
16. Zuo, Z.; Yang, Y.; Song, L.; Zhang, Z.; Jin, X. Characterization and Tribological Performance of Polyethersulfone/PTFE Compound Filled with Na-Montmorillonite. *Tribol. Lett.* **2021**, *69*, 138. [CrossRef]
17. Torokhov, V.G.; Chukov, D.I.; Tcherdyntsev, V.V.; Sherif, G.; Zadorozhnyy, M.Y.; Stepashkin, A.A.; Larin, I.I.; Medvedeva, E.V. Mechanical and Thermophysical Properties of Carbon Fiber-Reinforced Polyethersulfone. *Polymers* **2022**, *14*, 2956. [CrossRef]
18. Sharma, M.; Bijwe, J.; Singh, K. Studies for Wear Property Correlation for Carbon Fabric-Reinforced PES Composites. *Tribol. Lett.* **2011**, *43*, 267–273. [CrossRef]
19. Li, F.; Hua, Y.; Qu, C.B.; Xiao, H.M.; Fu, S.Y. Greatly enhanced cryogenic mechanical properties of short carbon fiber/polyethersulfone composites by graphene oxide coating. *Compos. Part A Appl. Sci. Manuf.* **2016**, *89*, 47–55. [CrossRef]
20. Veveris, A.A.; Kaloshkin, S.D. Production and Properties of Towpregs Based on Carbon Fibers Impregnated with Polyethersulfone by the Solution Method. *Inorg. Mater. Appl. Res.* **2025**, *16*, 1052–1056. [CrossRef]
21. Zhu, Y.; Shang, Y.; Zhang, H.; Ding, L.; Zhao, Y.; Han, Y.; Jiang, Z. Friction and wear properties of poly(ether sulfone) containing perfluorocarbon end group. *High Perform. Polym.* **2018**, *30*, 247–253. [CrossRef]
22. Sharma, M.; Bijwe, J. Influence of fiber–matrix adhesion and operating parameters on sliding wear performance of carbon fabric polyethersulphone composites. *Wear* **2011**, *271*, 2919–2927. [CrossRef]
23. Xue, Y.H.; Yan, S.C.; Chen, Y. Thermomechanical and tribological properties of polyimide and polyethersulfone blends reinforced with expanded graphite particles at various elevated tempera-tures. *J. Appl. Polym. Sci.* **2022**, *139*, 52512. [CrossRef]
24. Mamah, S.C.; Goh, P.S.; Ismail, A.F.; Suzaimi, N.D.; Yogarathinam, L.T.; Raji, Y.O.; El-badawy, T.H. Recent development in modification of polysulfone membrane for water treatment application. *J. Water Process Eng.* **2021**, *40*, 101835. [CrossRef]
25. Panin, S.V.; Luo, J.; Buslovich, D.G.; Alexeenko, V.O.; Berto, F.; Kornienko, L.A. Effect of Transfer Film on Tribological Properties of Anti-Friction PEI- and PI-Based Composites at Elevated Temperatures. *Polymers* **2022**, *14*, 1215. [CrossRef]
26. Yang, L.W.S.; Liu, W.; Xue, Q. An Investigation of the Friction and Wear Behaviors of Polyphenylene Sulfide Filled with Solid Lubricants. *Polym. Eng. Sci.* **2000**, *40*, 1825–1832. [CrossRef]
27. Zuo, Z.; Song, L.; Yang, Y. Tribological behavior of polyethersulfone-reinforced polytetra-fluoroethylene composite under dry sliding condition. *Tribol. Int.* **2015**, *86*, 17–27. [CrossRef]
28. Tarasov, S.Y.; Buslovich, D.G.; Panin, S.V.; Savchenko, N.L.; Kornienko, L.A.; Filatov, E.Y.; Moskvichev, E.N. Structure and tribological behavior of a polyetherimide/polytetrafluoroethylene matrix filled with negative thermal expansion zirconium tungstate particles. *Wear* **2024**, *558–559*, 205567. [CrossRef]
29. Cox, J.M.; Wright, B.A.; Wright, W.W. Thermal degradation of fluorine-containing polymers-1,2. *J. Appl. Polym. Sci.* **1964**, *8*, 2935–2961. [CrossRef]
30. Brown, E.N.; Rae, P.J.; Dattelbaum, D.M.; Clausen, B.; Brown, D.W. In-situ Measurement of Crystalline Lattice Strains in Polytetrafluoroethylene. *Exp. Mech.* **2008**, *48*, 119–131. [CrossRef]

31. Honda, Y.; Nishijima, S. Characterization of the melting process of PTFE using positron annihilation spectroscopy. *J. Phys. Conf. Ser.* **2015**, *618*, 012024. [CrossRef]
32. Luo, C.; Pei, J.; Zhuo, W.; Niu, Y.; Lia, G. The deformation mechanism and phase transition behavior of polytetrafluoroethylene Phase transition behavior and deformation mechanism of polytetrafluoroethylene under stretching. *RSC Adv.* **2021**, *11*, 39813. [CrossRef]
33. Shen, J.T.; Pei, Y.T.; De Hosson, J.T.M. Structural changes in polytetrafluoroethylene molecular chains upon sliding against steel. *J. Mater. Sci.* **2014**, *49*, 1484–1493. [CrossRef]
34. Gubanov, A.I.; Dedova, E.S.; Pavel, E.P.; Filatov, E.Y.; Kardash, T.Y.; Korenev, S.V.; Kulkov, S.N. Some peculiarities of zirconium tungstate synthesis by thermal decomposition of hydrothermal precursors. *Thermochim. Acta* **2014**, *597*, 19–26. [CrossRef]
35. Krasnov, A.P.; Shaposhnikova, V.V.; Salazkin, S.N.; Askadskii, A.A.; Goroshkov, M.V.; Naumkin, A.V. Effect of Chemical Structures of Heat-Resistant Tribostable Thermoplastics on Their Tribological Properties: Establishing a General Relationship. *INEOS OPEN* **2019**, *2*, 68–77. [CrossRef]
36. Evans, J.S.O.; Mary, T.A.; Vogt, T.; Subramanian, M.A.; Sleight, A.W. Negative Thermal Expansion in ZrW_2O_8 and HfW_2O_8. *Chem. Mater.* **1996**, *8*, 2809–2823. [CrossRef]
37. Amenta, F.; Bolelli, G.; D'Errico, F.; Ottani, F.; Pedrazzi, S.; Allesina, G.; Bertarini, A.; Puddu, P.; Lusvarghi, L. Tribological behavior of PTFE composites: Interplay between reinforcement type and counterface material. *Wear* **2022**, *510–511*, 204498. [CrossRef]
38. Hua, C.; Zhao, S.; Lin, L.; Schlarb, A.K. Tribological performance of a polyethersulfone (PESU)-based nanocomposite with potential surface changes of the metallic counterbody. *Appl. Surf. Sci.* **2023**, *636*, 157850. [CrossRef]

Disclaimer/Publisher's Note: The statements, opinions and data contained in all publications are solely those of the individual author(s) and contributor(s) and not of MDPI and/or the editor(s). MDPI and/or the editor(s) disclaim responsibility for any injury to people or property resulting from any ideas, methods, instructions or products referred to in the content.